

# Formation Flying Along Halo Orbit Using Switching Hamiltonian Structure-Preserving Control

Seungyun Jung\* and Youdan Kim\*<sup>†</sup>

\*Seoul National University

Seoul, 151-742, Republic of Korea

airwalk31@snu.ac.kr · ydkim@snu.ac.kr

<sup>†</sup>Corresponding author

## Abstract

Orbits for spacecraft formation flight along unstable orbit are designed. Hamiltonian structure-preserving (HSP) control is employed to stabilize the motion of spacecraft. Using a simple switching control strategy, the size of a circular orbit relative to a nominal trajectory can be systematically designed. By applying the switching HSP control repeatedly, station-keeping problem of a single spacecraft can be solved. The non-linear stability of the controller is analyzed by using Lagrange-Dirichlet criterion. Numerical simulation results show that the switching HSP controller works well in Earth-Moon system's  $L_2$  halo orbit.

## 1. Introduction

In recent years, spacecraft formation flying have been widely performed because the concept of the spacecraft formation flying has various advantages: reducing the cost, enhancing the system robustness and increasing the space observatory resolution. Most of research on the spacecraft formation flying have focused on Earth-centered missions, which are based on two-body problem called Keplerian orbit. However, as space mission requirements become complicated, the location of spacecraft are not restricted in the Earth orbit.

One of the most promising locations in the deep-space mission are libration points which are equilibria of the circular-restricted three-body problem (CR3BP). Around the libration points, there exist several families of orbits which are called Libration Point Orbit (LPO). There exist many research works on LPO based station-keeping problem.<sup>1</sup> Starting with ISEE-3, launched in 1978, a single spacecraft, for example, the Genesis, WMAP and Herchel have been already in LPO.

In recent years, not only a single spacecraft station-keeping problem but also a multiple spacecraft formation flying problem about a LPO has drawn much interest. NASA's planned missions, Terrestrial Planet Finder (TPF) and the Micro-Arcsecond X-ray Imaging Mission (MAXIM) are examples of multiple spacecraft formation flight. However, LPO is a non-Keplerian orbit, and therefore formation flying strategies based on Keplerian orbit cannot be applied. There are several research on LPO-based formation flying. Marchand et al.<sup>2</sup> investigated natural and non-natural formation flying in the vicinity of the LPO. Gurfil et al.<sup>3</sup> proposed a nonlinear adaptive neural control. Peng et al.<sup>4</sup> proposed an optimal periodic controller for formation flying on LPO. Impulsive control method was also studied by Qi et al.<sup>5</sup> Among the previous research, Scheeres et al.<sup>6</sup> presented a non-traditional continuous controller that achieves bounded motion, which is applicable to formation flying near the LPO. Because Scheeres' controller preserves the system's mathematical structure (symplectic Hamiltonian structure), it is called a Hamiltonian structure-preserving (HSP) controller. After Scheeres' work, there have been several research using HSP control. However, most of the previous research were focused only on stabilization, not on the shape of spacecraft formation pattern.

In this study, a simple switching HSP controller is suggested to stabilize the spacecraft and to make a circular relative trajectory whose radius size varies arbitrary. Numerical simulation is performed to demonstrate the effectiveness of the proposed controller.

## 2. Preliminaries

### 2.1 Dynamic Model of the CR3BP

The equations of motion in the CR3BP can be represented as<sup>7</sup>

$$\ddot{x} - 2\omega_f \dot{y} - x = -\frac{(1-\mu)(x+\mu)}{r_1^3} - \frac{\mu(x-1+\mu)}{r_2^3} \quad (1a)$$

$$\ddot{y} + 2\omega_f \dot{x} - y = -\frac{(1-\mu)y}{r_1^3} - \frac{\mu y}{r_2^3} \quad (1b)$$

$$\ddot{z} = -\frac{(1-\mu)z}{r_1^3} - \frac{\mu z}{r_2^3} \quad (1c)$$

where  $\bar{r} = (x, y, z)$  is a rotating frame of which the origin is the barycenter of the system. Conventionally, quantities in the CR3BP are normalized such that the distance between two primaries, as well as the mean motion  $\bar{\omega}_f = (0, 0, \omega_f)$  of the primaries, are both equal to a constant value of unity. In addition, the normalized mass unit is  $M = m_1 + m_2$ , and the mass ratio is  $\mu = m_2/M$ . Using the dimensionless units, the first primary is located on the  $x$ -axis at the point  $(-\mu, 0, 0)$ , while the second primary is at  $(1-\mu, 0, 0)$ . And,  $r_1 = [(x+\mu)^2 + y^2 + z^2]^{1/2}$  and  $r_2 = [(x-1+\mu)^2 + y^2 + z^2]^{1/2}$  are non-dimensional distances between primaries and spacecraft, respectively. Figure 1 shows the geometry of the CR3BP. The pseudo-potential function  $U(\bar{r})$  is defined as

$$U(\bar{r}) = V(\bar{r}) + \Phi(\bar{r}) \quad (2)$$

where  $V(\bar{r})$  is the gravitational potential function of two primaries, and  $\Phi(\bar{r})$  is the potential due to the rotation of the reference frame, which are defined as

$$V(\bar{r}) = \frac{1-\mu}{r_1} + \frac{\mu}{r_2} \quad (3a)$$

$$\Phi(\bar{r}) = \frac{1}{2}(\bar{\omega}_f \times \bar{r}) \cdot (\bar{\omega}_f \times \bar{r}) \quad (3b)$$

Then, the equations of motion can be rewritten as follows,

$$\ddot{x} - 2\omega_f \dot{y} = \nabla_x U(\bar{r}), \quad \ddot{y} + 2\omega_f \dot{x} = \nabla_y U(\bar{r}), \quad \ddot{z} = \nabla_z U(\bar{r}) \quad (4)$$

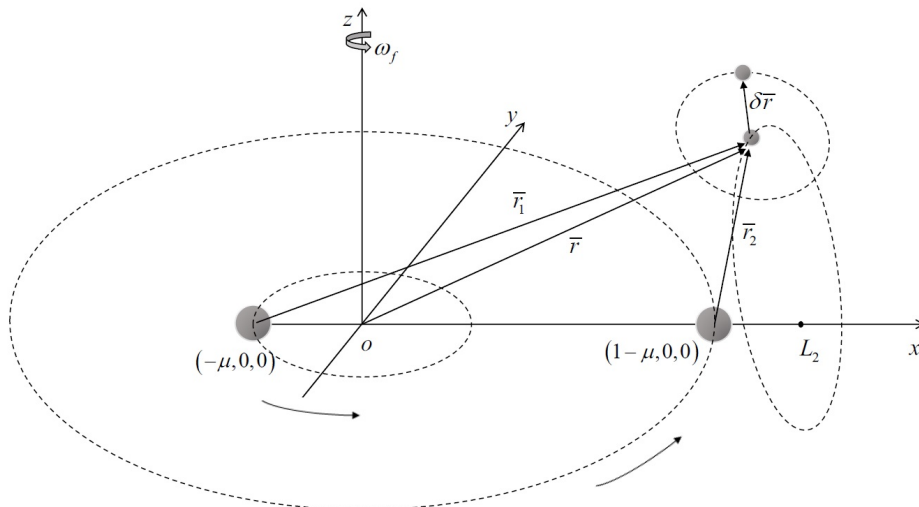


Figure 1: Geometry of the CR3BP and the spacecraft formation

The equilibrium points of the CR3BP can be obtained by solving  $\nabla U(\bar{r}) = 0$  in Eq. (4) with  $\dot{\bar{r}} = \ddot{\bar{r}} = 0$ . In Earth-Moon system case, there are five equilibrium points (also known as libration points), including three collinear points

that lie along the  $x$ -axis and two equilateral points. Linearization about any collinear equilibrium point reveals an eigenvalue structure of the type (hyperbolic) $\times$ (center) $\times$ (center).<sup>8</sup> It is well known that there are infinite number of periodic/quasi-periodic unstable orbits around the libration points, which are called LPO. Halo and Lissajous orbits are special periodic and quasi-periodic orbits around the collinear libration points. Figure 2 shows a halo orbit around the  $L_2$  point in the Earth-Moon system. The main objective of this study is to design a new type of spacecraft station-keeping and formation flying method along the orbits of these libration points.

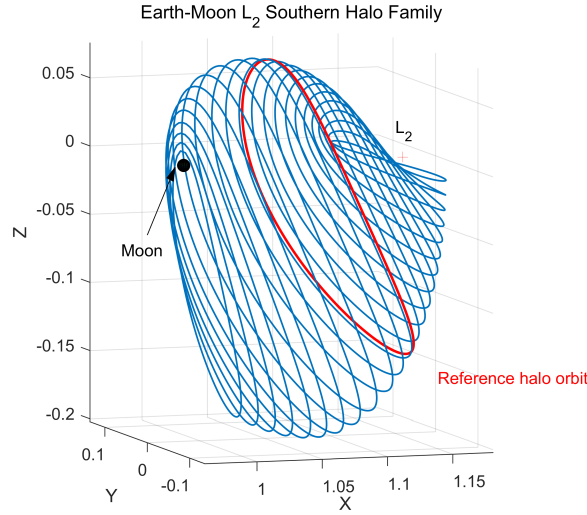


Figure 2: Southern halo family near the  $L_2$  Earth-Moon libration point

## 2.2 Hamiltonian Dynamics

Equation (4) can be also derived using Euler-Lagrange equation with a Lagrangian

$$\mathcal{L}(\bar{r}, \dot{\bar{r}}) = \frac{1}{2} \{ (\dot{x} - \omega_f y)^2 + (\dot{y} + \omega_f x)^2 + \dot{z}^2 \} + \frac{1-\mu}{r_1} + \frac{\mu}{r_2} \quad (5)$$

If the equation of motion is derived using the Lagrangian, then it has a Lagrangian structure. Let us consider a Legendre transformation.

$$\begin{bmatrix} \bar{q} \\ \bar{p} \end{bmatrix} = \begin{bmatrix} I_3 & 0_3 \\ -\omega_f J & I_3 \end{bmatrix} \begin{bmatrix} \bar{r} \\ \dot{\bar{r}} \end{bmatrix} \quad \text{where} \quad J = \begin{bmatrix} 0 & 1 & 0 \\ -1 & 0 & 0 \\ 0 & 0 & 0 \end{bmatrix} \quad (6)$$

Then, Eq. (4) can be transformed into the canonical Hamiltonian system form.

$$\dot{q}_1 = \frac{\partial H}{\partial p_1} = p_1 + \omega_f q_2 \quad , \quad \dot{p}_1 = -\frac{\partial H}{\partial q_1} = \omega_f p_2 - \frac{(1-\mu)(q_1 + \mu)}{r_1^3} - \frac{\mu(\mu + q_1 - 1)}{r_2^3} \quad (7a)$$

$$\dot{q}_2 = \frac{\partial H}{\partial p_2} = p_2 - \omega_f q_1 \quad , \quad \dot{p}_2 = -\frac{\partial H}{\partial q_2} = -\omega_f p_1 - \frac{(1-\mu)q_2}{r_1^3} - \frac{\mu q_2}{r_2^3} \quad (7b)$$

$$\dot{q}_3 = \frac{\partial H}{\partial p_3} = p_3 \quad , \quad \dot{p}_3 = -\frac{\partial H}{\partial q_3} = -\frac{(1-\mu)q_3}{r_1^3} - \frac{\mu q_3}{r_2^3} \quad (7c)$$

with the following Hamiltonian function.

$$\begin{aligned} H(\bar{q}, \bar{p}) &= \frac{1}{2} \bar{p}^T \bar{p} + \omega_f \bar{p}^T J \bar{q} + \frac{1}{2} \omega_f^2 \bar{q}(1:2)^T \bar{q}(1:2) - U(\bar{q}) \\ &= \frac{1}{2} (p_1^2 + p_2^2 + p_3^2) + \omega_f (p_1 q_2 - p_2 q_1) - \frac{1-\mu}{r_1} - \frac{\mu}{r_2} \end{aligned} \quad (8)$$

In the dynamical system point of view, CR3BP can be classified as a Hamiltonian systems. One of the important characteristics of the Hamiltonian systems is that vector fields governed by Hamilton's equations are volume-preserving. In other words, Hamiltonian system cannot have an asymptotic stable equilibrium point by nature.

### 3. Hamiltonian structure-preserving control

The concept of Hamiltonian structure-preserving(HSP) control was suggested by Scheeres et al.<sup>6</sup> whose work focused on Sun-Earth system halo orbit around the  $L_2$  point. HSP control uses the eigenstructure of the linearized equations of motion, evaluated along the orbit. Originally, the suggested HSP controller uses projected components of the position error along stable/unstable manifolds. By compensating the stable/unstable components of the position errors, it creates an artificial center manifold, as the eigenvalues of the linearized system are located on the imaginary axis. Although stabilization of the relative motion over a short time does not guarantee the orbit stability, Scheeres et al. showed that the orbit stability can be achieved when control gain is high. HSP control have been widely applied to stabilization of spacecraft on a solar sail,<sup>9</sup>  $J_2$ -perturbed mean circular orbit,<sup>10</sup> elliptic orbit,<sup>11</sup> quasi-halo orbit,<sup>12</sup> and high-amplitude distant prograde orbits.<sup>13</sup> Because HSP control makes the system marginally stable not asymptotically stable, the resulting motion of HSP control is a bounded trajectory (not converging trajectory). Due to the HSP control's feature, it is difficult to design the relative trajectory of the spacecraft because it cannot make the spacecraft converge to specific points or trajectories. In other words, using the HSP control, it is hard to make the spacecraft track the reference orbit. As a result, all of the previous research focused on only stabilization, not on shape of spacecraft relative motion. In this study a simple switching HSP controller is suggested to stabilize the spacecraft and to make a circular relative trajectory whose radius size varies arbitrary.

#### 3.1 Linear HSP controller design

The relative distance between two spacecrafts is usually very small compared with  $r_1$  and  $r_2$ , and therefore linearization is a useful approximation. Linearization of equation (4) with respect to a libration point leads to a linear time invariant system. However, linearization of equation (4) along a LPO results in a linear time varying system. Therefore, controller design for an orbit maintenance or formation flying along the orbit should be based on the linear time varying system model. Proceeding with the nonlinear equation (4), the periodic reference orbit can be defined as  $\bar{R}_r = [x_r, y_r, z_r]^T$  with the property  $\bar{R}_r(t+T) = \bar{R}_r(t)$  and velocity  $\bar{V}_r(t+T) = \bar{V}_r(t)$ . Let us define a real trajectory, which can be written as  $\bar{R} = [x, y, z]^T$  and  $\bar{V} = [\dot{x}, \dot{y}, \dot{z}]^T$ , and system state vector is defined as  $\bar{X} = [\bar{R}, \bar{V}]^T$ . Then, the small deviations of the real trajectory of the spacecraft from the reference orbit can be defined as

$$\delta\bar{X} = \bar{X} - \bar{X}_r \quad (9)$$

$$\delta\dot{\bar{X}} = \dot{\bar{X}} - \dot{\bar{X}}_r \approx A(t)\delta\bar{X} \quad (10)$$

$$A(t) = \begin{bmatrix} 0_3 & I_3 \\ U_{RR} & 2\omega_f J \end{bmatrix} \quad (11)$$

where  $U_{RR}$  is the second derivative of the pseudo-potential function in equation (2), and  $2\omega_f J$  is the term related to the Coriolis acceleration. Because the linearized equation (10) is also a Hamiltonian system. Equation (10) can be transformed to linear Hamiltonian system using a Legendre transformation.

$$\frac{d}{dt} \begin{bmatrix} \delta\bar{q} \\ \delta\bar{p} \end{bmatrix} = \begin{bmatrix} I_3 & 0_3 \\ -\omega_f J & I_3 \end{bmatrix} \begin{bmatrix} 0_3 & I_3 \\ U_{RR} & 2\omega_f J \end{bmatrix} \begin{bmatrix} I_3 & 0_3 \\ -\omega_f J & I_3 \end{bmatrix}^{-1} \begin{bmatrix} \delta\bar{q} \\ \delta\bar{p} \end{bmatrix} \quad (12)$$

with following Hamiltonian function

$$\begin{aligned} H_2(\delta\bar{q}, \delta\bar{p}) &= \frac{1}{2} \begin{bmatrix} \delta\bar{q}^T & \delta\bar{p}^T \end{bmatrix} \begin{bmatrix} 0_3 & -I_3 \\ I_3 & 0_3 \end{bmatrix} \begin{bmatrix} I_3 & 0_3 \\ -\omega_f J & I_3 \end{bmatrix} \begin{bmatrix} 0_3 & I_3 \\ U_{RR} & 2\omega_f J \end{bmatrix} \begin{bmatrix} I_3 & 0_3 \\ -\omega_f J & I_3 \end{bmatrix}^{-1} \begin{bmatrix} \delta\bar{q} \\ \delta\bar{p} \end{bmatrix} \\ &= \frac{1}{2} \begin{bmatrix} \delta\bar{q}^T & \delta\bar{p}^T \end{bmatrix} \begin{bmatrix} -U_{RR} - \omega_f^2 J J & -\omega_f J \\ \omega_f J & I_3 \end{bmatrix} \begin{bmatrix} \delta\bar{q} \\ \delta\bar{p} \end{bmatrix} \end{aligned} \quad (13)$$

Using equation (10), a linearized motion about a LPO can be written as

$$\delta\ddot{\bar{r}} - 2\omega_f J \delta\dot{\bar{r}} - U_{RR} \delta\bar{r} = 0 \quad (14)$$

Previous study<sup>6</sup> proved that if the reference orbit is cut for a very short time interval, then each orbit piece can be treated as a time invariant system. In other words,  $U_{RR}$  can be treated as a constant in a short time interval. Based on the knowledge of a linear time invariant system, a linear feedback control input can be designed as

$$T_c = T\delta\bar{r} + K\delta\dot{\bar{r}} \quad (15)$$

Then, the equation of motion in the closed loop system can be written as

$$\delta\ddot{\bar{r}} - (2\omega_f J + K)\delta\dot{\bar{r}} - (U_{RR} + T)\delta\bar{r} = 0 \quad (16)$$

Equation (16) can be simplified as a following form

$$\delta\ddot{\bar{r}} - S\delta\dot{\bar{r}} - \tilde{U}\delta\bar{r} = 0 \quad (17)$$

where  $S \triangleq 2\omega_f J + K$ , and  $\tilde{U} \triangleq U_{RR} + T$ .

Control input conditions preserving the symplectic Hamiltonian structure are as follow: i)  $T$  is a symmetric matrix, ii)  $K$  is skew symmetric matrix. Note that the controller forms of previous works<sup>6,9,13</sup> are examples of feedback control law satisfy above conditions. Therefore, it is unnecessary to restrict the controller form like previous research. Hsiao et al.<sup>14</sup> pointed out that if conditions of  $\tilde{U}$  and  $S$  for stable relative motions are found, then the control input can be obtained by simply subtracting  $U_{RR}$  and  $2\omega_f J$  from the desired  $\tilde{U}$  and  $S$ . Therefore, in this study, let us concentrate on finding the condition for stable relative motion rather than proposing a specific controller form.

Negative definiteness of  $\tilde{U}$  is a sufficient condition for the stability of the equilibrium points in linear sense. Assume that the controlled equations of motion can be made as follows

$$\delta\ddot{\bar{r}} - \tilde{U}\delta\bar{r} = 0 \quad (18)$$

with a negative definite matrix  $\tilde{U}$ . Then, the relative motion can be considered as a combination of three simple harmonic oscillations. Because  $\tilde{U}$  is symmetric,  $\tilde{U}$  is always diagonalizable as follows

$$\tilde{U} = M\Lambda M^{-1} \quad (19)$$

where  $M$  is an eigenvector matrix of the  $\tilde{U}$ , and  $\Lambda$  is a diagonalized matrix of  $\tilde{U}$ . Equation (18) can be rewritten as

$$\delta\ddot{\bar{r}} - M\Lambda M^{-1}\delta\bar{r} = 0 \quad (20)$$

Let us define a new variable  $\delta\bar{g} \triangleq M^{-1}\delta\bar{r}$ , then, equation (20) can be rewritten as

$$\delta\ddot{\bar{g}} - \Lambda\delta\bar{g} = 0 \quad (21)$$

where  $\delta\bar{g}$  is a new representation of  $\delta\bar{r}$  with respect to eigenvector matrix  $M$ . It is clear that equation (21) provides a simple harmonic oscillation. Due to the symmetry of  $\tilde{U}$  matrix, the eigenvector matrix  $M$  is orthonormal. In other words,  $\delta\bar{g}$ , which is the new representation of  $\delta\bar{r}$ , does not affect on an orthogonality of  $\delta\bar{r}$  in the phase space. Therefore, all of the remaining orbital motion analysis can be performed based on the basis which are the eigenvector of the  $\tilde{U}$  matrix.

### 3.2 Switching HSP controller design

If HSP control can make the equations of motion as Eq. (18), it is clear that the relative motion of deputy spacecraft is a combination of three simple harmonic oscillations. The relative motion of the deputy can be written as follows

$$\begin{aligned} \delta\bar{r}(t) &= M \cdot \begin{bmatrix} \delta g_1(t) \\ \delta g_2(t) \\ \delta g_3(t) \end{bmatrix} \\ &= [\bar{h}_1, \bar{h}_2, \bar{h}_3] \cdot \begin{bmatrix} \delta g_1(t) \\ \delta g_2(t) \\ \delta g_3(t) \end{bmatrix} = \sum_{i=1}^3 [\delta g_i(t) \cdot \bar{h}_i] = \sum_{i=1}^3 \left[ \{A_i \cos(\omega_i t) + B_i \sin(\omega_i t)\} \bar{h}_i \right] \end{aligned} \quad (22)$$

where  $A_i$  and  $B_i$  are constant coefficients,  $\omega_i^2$  is the magnitude of the eigenvalues of the  $\tilde{U}$  and  $\bar{h}_i$  is the eigenvectors of the  $\tilde{U}$ . Hsiao et al.<sup>15</sup> showed that the trajectory described by each oscillation mode forms an elliptical orbit with origin of frame at the center. Accordingly, the real relative trajectory is a linear combination of three elliptical orbits. Generally, it is difficult to imagine the real trajectories which are the combinations of three elliptical orbits. However, if a proper initial conditions and mode frequencies, i.e., eigenvalues, are given, the real trajectory (combined result of each mode) can be an elliptical/circular orbit. If the exact conditions making the real trajectory elliptical/circular orbit are known using that knowledge, then it is possible to design a switching HSP controller. With the switching controller, the size of elliptic/circular orbit can be changed systematically. In addition, a switching control is used repeatedly, the

## FORMATION FLYING ALONG HALO ORBIT USING SWITCHING HSP CONTROL

position convergence about the reference orbit can be achieved. Note that Liberzon et al.<sup>16,17</sup> provided a basic idea of asymptotic stabilization using a state-dependent switching control. They discussed the stabilizing switching strategy for the harmonic oscillator which is applicable to the HSP controller.

In this study, following cases will be discussed: i) transfer from a circular orbit with radius  $R_1$  to an elliptical orbit whose apsis distances are  $R_1$  and  $R_2$ , respectively, and ii) from an elliptical orbit whose apsis distances are  $R_1$  and  $R_2$  to a circular orbit with radius  $R_2$ . The basic concept of the switching HSP control is similar to Hohmann transfer. Firstly, let us assume that the deputy spacecraft rotates a circular orbit with radius  $R_1$ . At any point on the circular orbit, deputy spacecraft switches the HSP controller to transfer to the elliptical orbit, whose apsis distances are  $R_1$  and  $R_2$ , respectively. After transferring to the elliptical orbit, the spacecraft switches the HSP controller again at the other apsis to transfer to the circular orbit whose radius is  $R_2$ . By following these two step switching, it is possible to resize the deputy's circular orbit. For try switching strategy, it is required to know the orbital properties of the deputy spacecraft.

### 3.2.1 Orbital Properties of deputy spacecraft

Differentiating equation (22) with respect to  $t$  gives the relative velocity vector as

$$\delta\dot{\bar{r}}(t) = \sum_{i=1}^3 \left[ \{-A_i\omega_i \sin(\omega_i t) + B_i\omega_i \cos(\omega_i t)\} \bar{h}_i \right] \quad (23)$$

First of all, to make a real trajectory elliptical/circular orbit, each mode frequency should be same ( $\omega_i = \omega$ ). If the real trajectory is an elliptical orbit, the position and velocity vector will be perpendicular each other at the periapsis or apoapsis. By defining the apsis angle variable  $\theta_{\perp}$ , a following equation will hold.

$$\begin{aligned} \delta\bar{r}(t_{aps}) \cdot \delta\dot{\bar{r}}(t_{aps}) &= \left( \sum_{i=1}^3 \left[ \{A_i \cos(\theta_{\perp}) + B_i \sin(\theta_{\perp})\} \bar{h}_i \right] \right) \cdot \left( \sum_{i=1}^3 \left[ \omega \{-A_i \sin(\theta_{\perp}) + B_i \cos(\theta_{\perp})\} \bar{h}_i \right] \right) \\ &= \frac{\omega}{2} \left\{ \sum_{i=1}^3 (-A_i^2 + B_i^2) \right\} \sin(2\theta_{\perp}) + \omega \left\{ \sum_{i=1}^3 (A_i B_i) \right\} \cos(2\theta_{\perp}) \equiv 0 \end{aligned} \quad (24)$$

Therefore, we have

$$\cos(2\theta_{\perp}) = \pm \frac{\sum_{i=1}^3 (A_i^2 - B_i^2)}{\sqrt{\left\{ \sum_{i=1}^3 (A_i^2 - B_i^2) \right\}^2 + 4 \left\{ \sum_{i=1}^3 (A_i B_i) \right\}^2}} \quad (25)$$

$$\sin(2\theta_{\perp}) = \pm \frac{2 \left\{ \sum_{i=1}^3 (A_i B_i) \right\}}{\sqrt{\left\{ \sum_{i=1}^3 (A_i^2 - B_i^2) \right\}^2 + 4 \left\{ \sum_{i=1}^3 (A_i B_i) \right\}^2}} \quad (26)$$

Periapsis and apoapsis distances are represented as follows

$$\begin{aligned} |\delta\bar{r}(t_{aps})|^2 &= \left( \sum_{i=1}^3 \left[ \{A_i \cos(\theta_{\perp}) + B_i \sin(\theta_{\perp})\} \bar{h}_i \right] \right) \cdot \left( \sum_{i=1}^3 \left[ \{A_i \cos(\theta_{\perp}) + B_i \sin(\theta_{\perp})\} \bar{h}_i \right] \right) \\ &= \frac{1}{2} \left\{ \sum_{i=1}^3 (A_i^2 + B_i^2) \right\} \pm \frac{\frac{1}{2} \left\{ \sum_{i=1}^3 (A_i^2 - B_i^2) \right\}^2 + 2 \left\{ \sum_{i=1}^3 (A_i B_i) \right\}^2}{\sqrt{\left\{ \sum_{i=1}^3 (A_i^2 - B_i^2) \right\}^2 + 4 \left\{ \sum_{i=1}^3 (A_i B_i) \right\}^2}} \end{aligned} \quad (27)$$

Because the coefficients of each mode,  $A_i$  and  $B_i$ , are determined by the initial conditions, the distance of apsis can be also determined by given initial conditions.

### 3.2.2 Switching Point 1: From circular orbit to elliptical orbit

Under the equation of motion (18) with mode frequency  $\omega$  at any point on the circular orbit (with radius  $R_1$ ), the position and velocity of the spacecraft are expressed as equations (22) and (23). Assuming that the time at switching

point is  $t = 0$ , the position and velocity vector can be expressed as follows

$$\delta\bar{r}(0) = \sum_{i=1}^3 (A_i \bar{h}_i) \quad (28a)$$

$$\delta\dot{\bar{r}}(0) = \omega \sum_{i=1}^3 (B_i \bar{h}_i) \quad (28b)$$

The objective is to transfer the spacecraft from a circular orbit to an elliptical orbit whose target apsis distance is  $R_2$ . After switching, the equation of motion become equation (18) with new mode frequency  $\omega_1$ . Under this switched equation of motion, the position and velocity of the spacecraft can be expressed as follows

$$\delta\bar{r}(0) = \sum_{i=1}^3 \left[ \{C_i \cos(\omega_1 t) + D_i \sin(\omega_1 t)\} \bar{h}_i \right] \quad (29a)$$

$$\delta\dot{\bar{r}}(0) = \omega \sum_{i=1}^3 \left[ \{-C_i \omega_1 \sin(\omega_1 t) + D_i \omega_1 \cos(\omega_1 t)\} \bar{h}_i \right] \quad (29b)$$

Then, we have

$$\delta\bar{r}(0) = \sum_{i=1}^3 (C_i \bar{h}_i) \quad (30a)$$

$$\delta\dot{\bar{r}}(0) = \omega_1 \sum_{i=1}^3 (D_i \bar{h}_i) \quad (30b)$$

At the switching point, the position and velocity vectors should be same, and therefore following equations can be obtained.

$$A_i = C_i \quad , \quad \omega B_i = \omega_1 D_i \quad (31)$$

In addition, if  $\omega_1 = k\omega$  ( $k$  is real number), then  $D_i = B_i/k$ . Under these relations, the periapsis and apoapsis distances can be expressed as follows

$$\begin{aligned} |\delta\bar{r}(t_{aps})|^2 &= \frac{1}{2} \left\{ \sum_{i=1}^3 (C_i^2 + D_i^2) \right\} \pm \frac{\left[ \frac{1}{2} \left\{ \sum_{i=1}^3 (C_i^2 - D_i^2) \right\}^2 + 2 \left\{ \sum_{i=1}^3 (C_i D_i) \right\}^2 \right]}{\sqrt{\left\{ \sum_{i=1}^3 (C_i^2 - D_i^2) \right\}^2 + 4 \left\{ \sum_{i=1}^3 (C_i D_i) \right\}^2}} \\ &= \frac{1}{2} \left\{ \sum_{i=1}^3 \left( A_i^2 + \frac{B_i^2}{k^2} \right) \right\} \pm \frac{\left[ \frac{1}{2} \left\{ \sum_{i=1}^3 \left( A_i^2 - \frac{B_i^2}{k^2} \right) \right\}^2 + 2 \left\{ \sum_{i=1}^3 \left( \frac{A_i B_i}{k} \right) \right\}^2 \right]}{\sqrt{\left\{ \sum_{i=1}^3 \left( A_i^2 - \frac{B_i^2}{k^2} \right) \right\}^2 + 4 \left\{ \sum_{i=1}^3 \left( \frac{A_i B_i}{k} \right) \right\}^2}} \end{aligned} \quad (32)$$

After plugging the desired apsis value,  $R_2$ , in the left hand side of equation (32), equation (32) is solved numerically to get the  $k$  value. Then, switched system's mode frequency can be determined by  $\omega_1 = k\omega$ . Finally, the HSP controller can be constructed as follows

$$\begin{aligned} T_{c1} &= T\delta\bar{r} + K\delta\dot{\bar{r}} \\ &= (M\Lambda_1 M^{-1} - U_{RR})\delta\bar{r} - 2\omega_f J\delta\dot{\bar{r}} \\ &= (-\omega_1^2 I_3 - U_{RR})\delta\bar{r} - 2\omega_f J\delta\dot{\bar{r}} \end{aligned} \quad (33)$$

### 3.2.3 Switching Point 2: From elliptical orbit to circular orbit

The second switching strategy is used when the spacecraft traveling along the elliptical orbit reaches the other apsis. Assume that, after the second switching, the equation of motion is equation (18) with new mode frequency  $\omega_2$ . Then, it is designed that the motion of the switched system is a circular orbit (with radius  $R_2$ ). At the switching point, the position and velocity vectors are perpendicular each other, and therefore the remaining dynamics condition of the

## FORMATION FLYING ALONG HALO ORBIT USING SWITCHING HSP CONTROL

switched system to achieve the circular motion is the magnitude of acceleration. The magnitude of acceleration for the circular orbit is  $|\delta\ddot{r}| = |\delta\dot{r}|^2/|\delta\bar{r}|$ . By using the switched system's equations of motion  $\delta\ddot{r} - M\Lambda_2 M^{-1}\delta\bar{r} = 0$ , the following equations should hold for a circular motion.

$$|M\Lambda_2 M^{-1}\delta\bar{r}| = \omega_2^2 |\delta\bar{r}| \equiv \frac{|\delta\dot{r}|^2}{|\delta\bar{r}|} \quad (34)$$

Solving equation (34), a new mode frequency  $\omega_2$  can be obtained. Finally, the HSP controller can be constructed as follows

$$\begin{aligned} T_{c2} &= T\delta\bar{r} + K\delta\dot{\bar{r}} \\ &= (M\Lambda_2 M^{-1} - U_{RR})\delta\bar{r} - 2\omega_f J\delta\dot{\bar{r}} \\ &= (-\omega_2^2 I_3 - U_{RR})\delta\bar{r} - 2\omega_f J\delta\dot{\bar{r}} \end{aligned} \quad (35)$$

### 3.3 Stability of controller

#### 3.3.1 Nonlinear Stability

It is well-known that if a linearized system matrix has only pure imaginary eigenvalues, the Hartman-Grobman theorem cannot conclude nonlinear stability of the equilibrium points. Because HSP controller makes the topology type of the equilibrium change from hyperbolic to elliptic, a nonlinear stability of the stabilized equilibrium points is not guaranteed. Therefore, it is needed to prove the nonlinear stability of the HSP controller. Arnold's stability theorem can be applied to prove the nonlinear stability of the elliptic equilibrium in 2DOF system. However, Arnold's stability theorem cannot be applied to a 3DOF system and also does not guarantee the nonlinear stability in resonance condition. Xu et al.<sup>9</sup> showed the nonlinear stability of the controller with respect to an equilibrium point by the Morse lemma. In this study, the nonlinear stability of the HSP controller with respect to a periodic orbit is proved using Lagrange-Dirichlet criterion. The Lagrange-Dirichlet theorem is a general stability theorem for the equilibria of Hamiltonian systems.

**Theorem 1 (Lagrange-Dirichlet)** *If the second variation (Hessian) of the Hamiltonian, i.e.,  $H_{zz}$  with  $\bar{z} = (\bar{q}, \bar{p})$ , is definite at the nondegenerate critical point  $z^*$ , then the equilibrium point is stable.*<sup>18</sup>

Before applying the HSP control, Hamiltonian of the system is described as in Eq. (8). Then, controlled Hamiltonian ( $\hat{H}$ ) can be modified as

$$\begin{aligned} \hat{H}(\bar{q}, \bar{p}) &= \frac{1}{2}\bar{p}^T \bar{p} + \omega_f \bar{p}^T J\bar{q} + \Delta \bar{p}^T J\delta\bar{q} + \frac{1}{2}\Delta^2 \delta\bar{q}(1:2)^T \delta\bar{q}(1:2) + \Delta\omega_f \bar{q}(1:2)^T \delta\bar{q}(1:2) + \Delta\bar{q}^T J\dot{\bar{q}}^* - U(\bar{q}) \\ &+ \frac{1}{2}\omega_f^2 \bar{q}(1:2)^T \bar{q}(1:2) - \frac{1}{2}\delta\bar{q}^T T\delta\bar{q} \\ &= \frac{1}{2}(p_1^2 + p_2^2 + p_3^2) + \omega_f(-p_2q_1 + p_1q_2) + \Delta\left\{-p_2(q_1 - q_1^*) + p_1(q_2 - q_2^*)\right\} + \frac{1}{2}\Delta^2\left\{(q_1 - q_1^*)^2 + (q_2 - q_2^*)^2\right\} \\ &+ \Delta\left\{\omega_f q_1(q_1 - q_1^*) + \omega_f q_2(q_2 - q_2^*) + q_1\dot{q}_2^* - q_2\dot{q}_1^*\right\} - \left[\frac{1-\mu}{r_1} + \frac{\mu}{r_2}\right] - \frac{1}{2}\left\{T_{11}(q_1 - q_1^*)^2 + T_{22}(q_2 - q_2^*)^2\right. \\ &\left.+ T_{33}(q_3 - q_3^*)^2 + 2T_{12}(q_1 - q_1^*)(q_2 - q_2^*) + 2T_{13}(q_1 - q_1^*)(q_3 - q_3^*) + 2T_{23}(q_2 - q_2^*)(q_3 - q_3^*)\right\} \end{aligned} \quad (36)$$

where  $\Delta$  is the magnitude of feedback angular velocity of the frame. In other words,  $K = 2\Delta J$ . Then, Hessian of the controlled Hamiltonian can be written as follows

$$\nabla^2 \hat{H}(\bar{q}, \bar{p}) = \begin{bmatrix} & & & 0 & -(\omega_f + \Delta) & 0 \\ & B & & (\omega_f + \Delta) & 0 & 0 \\ & & & 0 & 0 & 0 \\ 0 & (\omega_f + \Delta) & 0 & 1 & 0 & 0 \\ -(\omega_f + \Delta) & 0 & 0 & 0 & 1 & 0 \\ 0 & 0 & 0 & 0 & 0 & 1 \end{bmatrix} \quad (37)$$

$$B = \begin{bmatrix} \frac{\partial^2 \hat{H}}{\partial q_1^2} & \frac{\partial^2 \hat{H}}{\partial q_2 \partial q_1} & \frac{\partial^2 \hat{H}}{\partial q_3 \partial q_1} \\ \frac{\partial^2 \hat{H}}{\partial q_1 \partial q_2} & \frac{\partial^2 \hat{H}}{\partial q_2^2} & \frac{\partial^2 \hat{H}}{\partial q_3 \partial q_2} \\ \frac{\partial^2 \hat{H}}{\partial q_1 \partial q_3} & \frac{\partial^2 \hat{H}}{\partial q_2 \partial q_3} & \frac{\partial^2 \hat{H}}{\partial q_3^2} \end{bmatrix} \quad (38)$$

## FORMATION FLYING ALONG HALO ORBIT USING SWITCHING HSP CONTROL

$$\frac{\partial^2 \tilde{H}}{\partial q_1^2} = 2\Delta\omega_f + \Delta^2 + \omega_f^2 - U_{xx} - T_{11} \quad (39a)$$

$$\frac{\partial^2 \tilde{H}}{\partial q_2^2} = 2\Delta\omega_f + \Delta^2 + \omega_f^2 - U_{yy} - T_{22} \quad (39b)$$

$$\frac{\partial^2 \tilde{H}}{\partial q_3^2} = -U_{zz} - T_{33} \quad (39c)$$

$$\frac{\partial^2 \tilde{H}}{\partial q_2 \partial q_1} = -U_{xy} - T_{12} \quad (39d)$$

$$\frac{\partial^2 \tilde{H}}{\partial q_3 \partial q_1} = -U_{xz} - T_{13} \quad (39e)$$

$$\frac{\partial^2 \tilde{H}}{\partial q_3 \partial q_2} = -U_{yz} - T_{23} \quad (39f)$$

Let us propose a control input as follows

$$\begin{aligned} T_c &= T\delta\bar{r} + K\delta\dot{\bar{r}} \\ &= (M\Lambda_{new}M^{-1} - U_{RR})\delta\bar{r} - 2\omega_f J\delta\dot{\bar{r}} \\ &= (-\omega_{new}^2 I_3 - U_{RR})\delta\bar{r} - 2\omega_f J\delta\dot{\bar{r}} \end{aligned} \quad (40)$$

Then, the magnitude of controlled angular velocity of the frame is zero ( $\omega_f + \Delta = 0$ ). Consequently, Hessian of the controlled Hamiltonian is a diagonal matrix. Because  $B$  has full rank at the equilibrium point, the Hessian of Hamiltonian also has full rank at the equilibrium point. Therefore, the equilibrium is nondegenerate and the Hessian of Hamiltonian is positive definite. In conclusion, by Lagrange-Dirichlet criterion, HSP controller is nonlinearly stable.

### 3.3.2 Orbit Stability

In contrast to autonomous systems, non-autonomous periodic system may be unstable even though the equilibrium is always stable during its period. Scheeres et al.<sup>6</sup> evaluated the orbit stability (= Lagrange stability) using Floquet theory and numerical integration. The orbit stability can be evaluated by computing the eigenvalues of the monodromy matrix. If all of the eigenvalues of the monodromy matrix reside on the unit circle in the complex plane, then the orbit motion is stable in the sense of Lagrange. For the spacecraft formation flying along the halo orbit, both Lyapunov stability and orbit stability should be satisfied. In this study, the orbit stability is also investigated.

## 4. Numerical Simulation

Table 1: System parameter values

Quantity	Value	Units
Gravitational constant	$6.674 \times 10^{-20}$	$km^3 kg^{-1} s^{-2}$
Earth mass ( $m_1$ )	$5.972 \times 10^{24}$	kg
Moon mass ( $m_2$ )	$7.347 \times 10^{22}$	kg
Mass parameter ( $\mu$ )	0.01215	N/A
Characteristic length ( $l^*$ )	385692.5	km
Characteristic Time ( $t^*$ )	4.364	days

Table 2: Reference halo orbit parameter values

Quantity	Value	Units
Z-amp.	-55154.03	km
Period	14	days
Jacobi constant	3.07607	N/A

## FORMATION FLYING ALONG HALO ORBIT USING SWITCHING HSP CONTROL

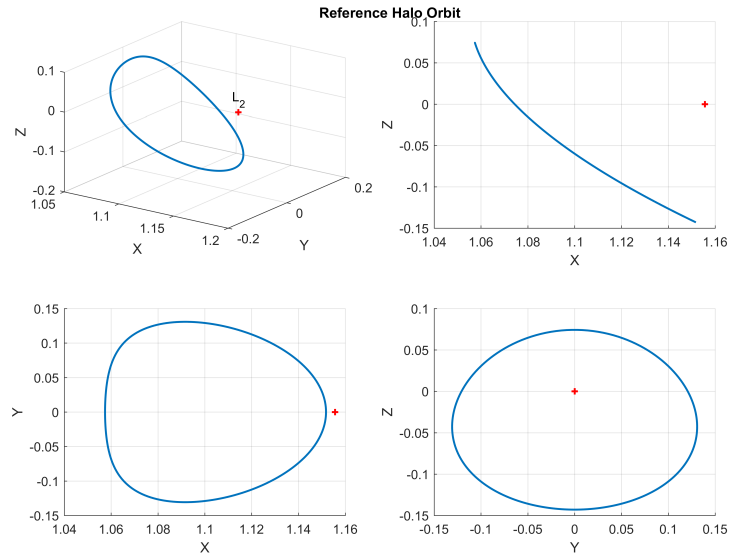


Figure 3: Reference Halo Orbit

System parameters used in the simulation are summarized in Table 1, and the properties of the reference halo orbit are summarized in Table 2. Radii of transfer orbits and the initial values of deputy spacecrafts are summarized in Table 3 and 4, respectively. The reference orbit is one of the potential orbits for coverage of the lunar south pole.<sup>19</sup> All the numerical simulations are conducted based on this reference orbit. Figure 4 7 show the numerical simulation results. Numerical simulations are performed using full nonlinear dynamics,  $\ddot{\vec{r}} - 2\omega_f J \dot{\vec{r}} = \nabla U(\vec{r}) + T_c$ , rather than using the linearized dynamics,  $\delta\ddot{\vec{r}} - 2\omega_f J \delta\dot{\vec{r}} = \nabla^2 U(\vec{r}) + T_c$ . Simulation results show that, by applying the switching HSP control, it is possible to change the size of circular motion of the deputy spacecraft. The switching process using piecewise simple harmonic oscillation was discussed by Liberzon.<sup>17</sup> Liberzon and Morse showed that even if piecewise system matrices are not asymptotic stable, asymptotic stabilization of the system could be achieved by using simple switching strategies. In our cases, switching strategy can also make position convergence to the reference trajectory. However, as the radius of circular orbit decreases, the rotating frequency increases. Therefore, convergence to the reference trajectory using switching HSP control is not efficient in fuel consumption point of view. Figure 8 shows that switching HSP controller works well when the location of the deputy spacecraft is far from the leader spacecraft. Note that the required distances for spacecraft formation flying mission are usually 1~100km.<sup>14,20</sup> Also, the magnitude of eigenvalues of monodromy matrix are all unity, and therefore orbit stability is guaranteed.

Table 3: Radius of transfer orbit

	Deputy 1	Deputy 2	Deputy 3
$R_1$ [m]	100	100	100
$R_2$ [m]	200	50	100

Table 4: Deputy spacecrafts initial value

Quantity	Value
Frequency ( $\omega$ )	70
Plane orientation ( $\vec{n}$ )	(1,1,1)
Deputy#1 position dir.	(1,1,-2)
Deputy#2 position dir.	(1,-2,1)
Deputy#3 position dir.	(-2,1,1)

## FORMATION FLYING ALONG HALO ORBIT USING SWITCHING HSP CONTROL

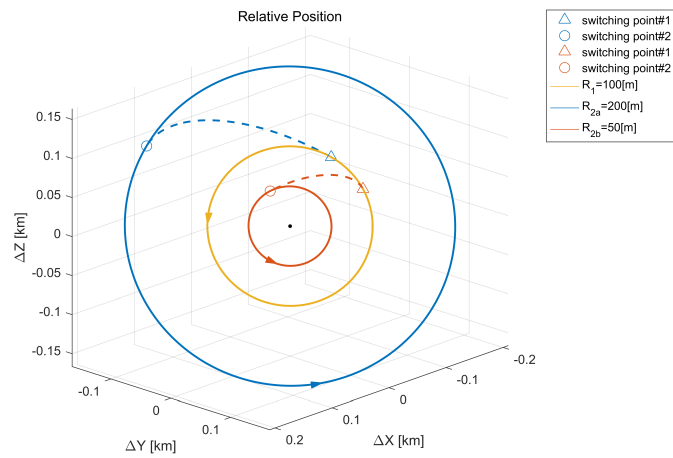
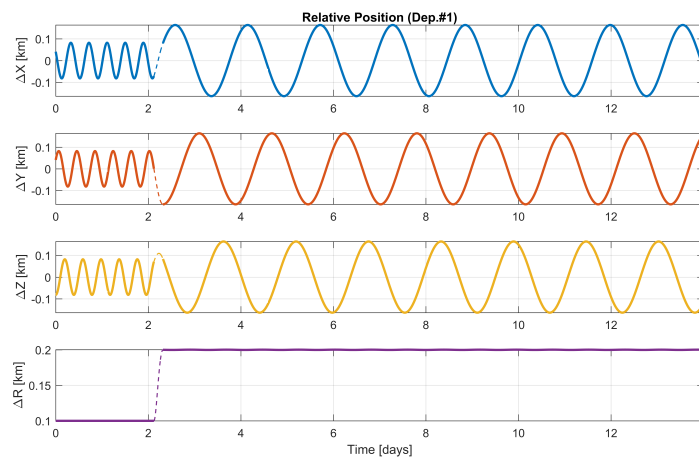
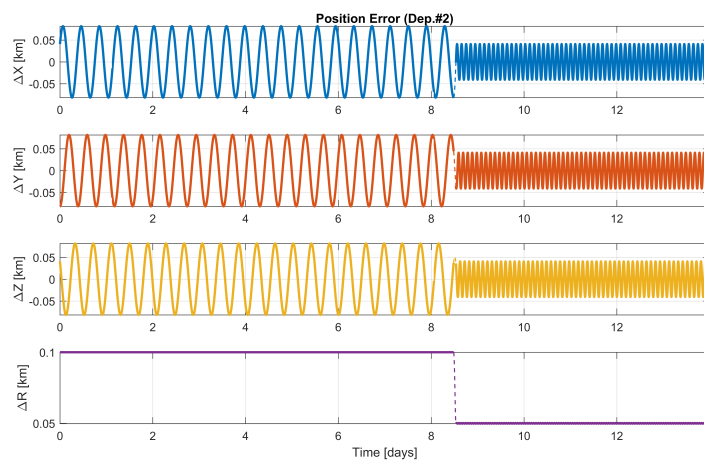
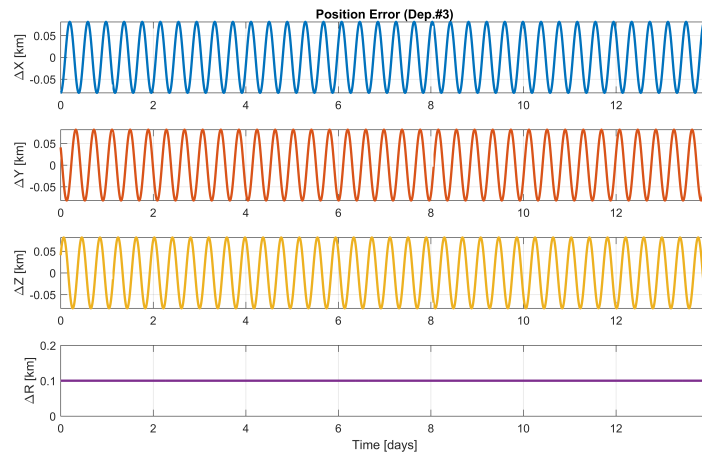
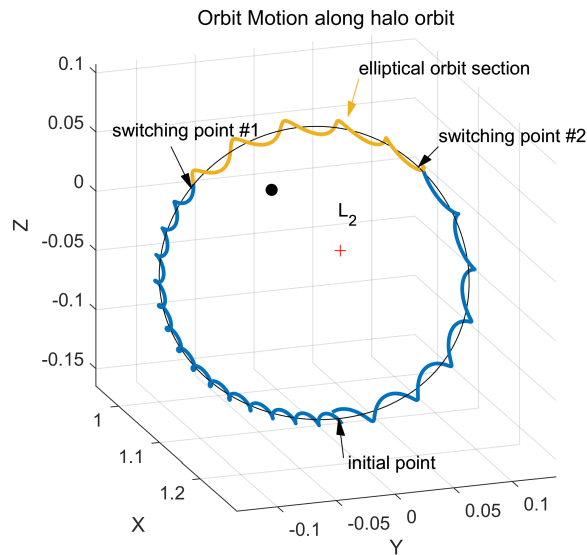


Figure 4: Orbit transfer using Switching HSP control (relative motion)

Figure 5: Relative Position of Deputy S/C #1 ( $R_1 = 100m \rightarrow R_2 = 200m$ )Figure 6: Relative Position of Deputy S/C #2 ( $R_1 = 100m \rightarrow R_2 = 50m$ )

## FORMATION FLYING ALONG HALO ORBIT USING SWITCHING HSP CONTROL

Figure 7: Relative Position of Deputy S/C #3 ( $R = 100m$ )Figure 8: Exaggerated Orbit size formation flying scenario along halo orbit ( $R_1 = 2000km \rightarrow R_2 = 3000km$ )

## 5. Conclusions

The original concept of the Hamiltonian structure-preserving control to design the elliptic/circular orbit pattern of spacecraft was extended by using simple switching control strategy. For targeting the desired apsis distance, the properties of orbit motion, which are very similar to Hohmann transfer strategy, are utilized. Proposed switching HSP controller can make the orbit size change to desired one systematically, which was impossible using previous HSP controllers. The nonlinear stability of the controller was analyzed using Lagrange-Dirichlet criterion. Numerical simulation are performed to demonstrate the performance of the switching Hamiltonian structure-preserving controller in usual formation flying ranges.

## 6. Acknowledgments

This work has been supported by the National GNSS Research Center program of Defense Acquisition Program Administration and Agency for Defense Development.

## References

- [1] M. Shirobokov, S. Trofimov, and M. Ovchinnikov. Survey of station-keeping techniques for libration point orbits. *Journal of Guidance, Control, and Dynamics*, 40(5):1085–1105, 2017.
- [2] B. G. Marchand and K. C. Howell. Control strategies for formation flight in the vicinity of the libration points. *Journal of Guidance, Control, and Dynamics*, 28(6):1210–1219, 2005.
- [3] P. Gurfil, M. Idan, and N. J. Kasdin. Adaptive neural control of deep-space formation flying. *Journal of Guidance, Control, and Dynamics*, 26(3):491–501, 2003.
- [4] H. Peng, J. Zhao, Z. Wu, and W. Zhong. Optimal periodic controller for the formation flying on libration point orbits. *Acta Astronautica*, 69(7-8):537–550, 2011.
- [5] R. Qi, S. Xu, and M. Xu. Impulsive control for formation flight about libration points. *Journal of Guidance, Control, and Dynamics*, 35(2):484–496, 2012.
- [6] D. J. Scheeres, F. Y. Hsiao, and N. X. Vinh. Stabilizing motion relative to an unstable orbit: Applications to spacecraft formation flight. *Journal of Guidance, Control, and Dynamics*, 26(1):62–73, 2003.
- [7] D. Cielaszyk and B. Wie. New approach to halo orbit determination and control. *Journal of Guidance, Control, and Dynamics*, 19(2):266–273, 1996.
- [8] A. Jorba and J. Masdemont. Dynamics in the center manifold of the collinear points of the restricted three body problem. *Physica D: Nonlinear Phenomena*, 132(1-2):189–213, 1999.
- [9] M. Xu and S. Xu. Structure-preserving stabilization for hamiltonian system and its applications in solar sail. *Journal of Guidance, Control, and Dynamics*, 32(3):997–1004, 2009.
- [10] M. Xu, J. Zhu, T. Tan, and S. Xu. Application of hamiltonian structure-preserving control to formation flying on a  $j_2$ -perturbed mean circular orbit. *Celestial Mechanics and Dynamical Astronomy*, 125(4):403–433, 2012.
- [11] M. Xu, Y. Liang, T. Tan, and L. Wei. Cluster flight control for fractionated spacecraft on an elliptic orbit. *Celestial Mechanics and Dynamical Astronomy*, 125(4):383–412, 2016.
- [12] M. Xu, Y. Liang, and X. Fu. Formation flying on quasi-halo orbits in restricted sun-earth/moon system. *Aerospace Science and Technology*, 67:118–125, 2017.
- [13] S. Soldini, C. Colombo, and Scott J. I. Walker. Solar radiation pressure hamiltonian feedback control for unstable libration-point orbits. *Journal of Guidance, Control, and Dynamics*, 40(6):1374–1389, 2017.
- [14] F. Y. Hsiao and D. J. Scheeres. Design of spacecraft formation orbits relative to a stabilized trajectory. *Journal of Guidance, Control, and Dynamics*, 28(4):782–794, 2005.
- [15] F. Y. Hsiao and D. J. Scheeres. The dynamics of formation flight about a stable trajectory. *The Journal of Astronautical Sciences*, 50(3):269–287, 2002.
- [16] D. Liberzon. *Switching in Systems and Control*. Springer, 2003.
- [17] D. Liberzon and A. S. Morse. Basic problems in stability and design of switched systems. *IEEE Control systems*, 19(5):59–70, 1999.
- [18] R. Krechetnikov and J. E. Marsden. Dissipation-induced instabilities in finite dimensions. *Reviews of Modern Physics*, 79(2):519–553, 2007.
- [19] D. J. Grebow, M. T. Ozimek, K. C. Howell, and D. C. Folta. Multibody orbit architectures for lunar south pole coverage. *Journal of Spacecraft and Rockets*, 45(2):344–358, 2008.
- [20] C. Beichman, G. Gomez, M. Lo, J. Masdemont, and L. Romans. Searching for life with the terrestrial planet finder: Lagrange point options for a formation flying interferometer. *Advances in Space Research*, 34(3):637–644, 2004.